Available online at www.sciencedirect.com
SCIENCE DIRECT®
Journal of Solid State Chemistry 178 (2005) 477–482
JOURNAL OF SOLID STATE CHEMISTRY
www.elsevier.com/locate/jssc

Preparation and characterization of optical spectroscopy of Lu_2O_3:Eu nanocrystals

Mei Xu[a,b], Weiping Zhang[b], Ning Dong[b], Yin Jiang[b], Ye Tao[c], Min Yin[b,*]

[a]*Structure Research Laboratory, University of Science and Technology of China, Hefei 230026, China*
[b]*Department of Physics, University of Science and Technology of China, Number 96, Jinzhai Road, Hefei City, Anhui Province 230026, China*
[c]*Beijing Synchrotron Radiation Facility, Institute of High Energy Physics, Beijing 100039, China*

Received 4 May 2004; received in revised form 16 September 2004; accepted 16 September 2004

Abstract

Nanoscale Lu_2O_3:Eu powders were prepared by solution combustion synthesis. X-ray diffraction (XRD), high-resolution electronic microscope (HREM), Fourier transform infrared spectroscopy (FT-IR), excitation and emission spectra, as well as fluorescent decay curves were measured to characterize the structure and luminescent properties of the samples. The results show that the compound of composition Lu_2O_3 crystallizes in pure cubic structure. By changing the ratio of glycine to nitrate in the combustion process, the particle size varies from 40 nm to less than 5 nm. The emission and excitation spectra strongly depend on the particle size of the samples. Novel emission band, red-shift of charge transfer band (CTB) and shortening of lifetime were observed in nanoscale samples.

Keywords: Nanocrystalline Lu_2O_3:Eu; Combustion synthesis; Photoluminescence; Amorphous phase

1. Introduction

As a method of ionizing-radiation-detection, scintillator materials have been widely used in the field of high-energy physics, nuclear physics, particle physics and medical imaging in the past few decades [1]. To meet the rapid development of modern science and technology, it is quite necessary to find new scintillator materials.

Recently, there has been a great growth of interest in lutetium-based compounds, such as lutetium silicate, lutetium aluminate and lutetium oxide [2–5]. High Z number ($Z = 71$), high physical and chemical stability and high luminescent efficiency make them very suitable for application in scintillator materials, especially medical ones. Rare-earth ions doped lutetium-based compounds have been applied in a wide range of fields, such as the detection of X-ray and γ particles [6].

Similar to the famous luminescence host material Y_2O_3, Lu_2O_3 always crystallizes in cubic structure with high symmetry and high stability. There are two symmetric sites for Lu^{3+} ion in cubic Lu_2O_3: C_2 and S_6. When doped into the Lu_2O_3 host, the RE ions take the place of Lu^{3+} on these two sites in a certain ratio. Lu_2O_3 has a high density of 9.4 g/cm^3, which is highly suitable for medical imaging use. But the melting point of Lu_2O_3 is as high as 2450 °C, and the single crystal is usually grown by using the Czochralski technique in a iridium crucible. It is an expensive, time-consuming and size-limiting process. Finding the substitute for single crystal becomes one of the focuses of recent researches. Zych [7] and Lempicki et al. [8] have carried out the method of hot pressing and vacuum sintering to make transparent ceramic from polycrystalline powders. This method can greatly decrease the synthesis temperature from the melting point of Lu_2O_3 (2450 °C) to about

*Corresponding author. Fax: +86 551 360 1073.
E-mail address: yinmin@ustc.edu.cn (M. Yin).

0022-4596/$ - see front matter © 2004 Elsevier Inc. All rights reserved.
doi:10.1016/j.jssc.2004.09.003

1700 °C. It has shown some prospect in preparing ceramic that may partially replace single crystal in wide-range applications.

In order to get high-quality ceramic, it is important to make crystalline powders with good performance as precursors. In the past decades, researchers took great interest in nanoscale materials and found that the properties of nanocrystalline phosphors are usually different from their bulk counterparts because of the high surface-to-volume ratio and the quantum effect. Nanophosphors have some luminescent properties that are superior to bulk materials of the same components, such as the coexistence of high quenching concentration and high luminescent efficiency [9], and have been studied widely in both fundamental researches and practical applications.

Solution combustion synthesis is a method that has been widely used in preparation of luminescent materials, including nanoscale phosphors. It produces remarkably fine and homogeneous powders with high chemical purity and high specific surface, which enable them suitable to be hot-pressed and then vacuum sintered to make transparent ceramic a challenger to single crystal.

In the present work we report the combustion synthesis and luminescent properties of Eu^{3+} doped Lu_2O_3 nanopowders.

2. Experimental

Nanocrystalline Lu_2O_3:Eu powder was prepared by a nitrate-glycine combustion synthesis (CS) process. Starting materials are Lu_2O_3 (4N), Eu_2O_3 (4N), nitric acid (AR) and glycine (AR). Lu_2O_3 and Eu_2O_3 were dissolved in nitric acid, and glycine in deionized water, respectively. These reagents were mixed in an appropriate ratio and stirred adequately to make the precursor solution, which was then heated in a porcelain crucible. With the evaporation of excess free water, the solution was concentrated and bubbled up. When the water was almost dried, the temperature of the system rose quickly, and then the reactant was enkindled and the combustion self-propagated from the ignition spot throughout the whole reactant system. The combustion process was extremely vigorous with a large amount of gas giving off. The residual white ash was the expected nanocrystalline Lu_2O_3:Eu. The reaction is as follows:

$$6(1-x)Lu(NO_3)_3 + 6xEu(NO_3)_3 + 10C_2H_5NO_2 + 28O_2 \rightarrow 3(Lu_{1-x}Eu_x)_2O_3 + 20CO_2 + 25H_2O + 28NO_2. \quad (1)$$

In our earlier work we found that the glycine-to-nitrate ratio (G/N) always influences the temperature of the flame in the combustion process and thus the particle size and properties of products [10,11]. In this work, the value of G/N was adjusted to be stoichiometric (0.56, Sample A) and oxidant-rich (0.39, 0.33, 0.28, Samples B, C, D). The most vigorous combustion was observed in the case of G/N = 0.56 (sample A). The Eu^{3+} concentration is 2 at% for all the samples.

The XRD patterns of the samples were recorded by an MAC Science Co. Ltd MXP18AHF rotation anode X-ray diffractometer with Cu $K\alpha$ radiation. The morphologies of the samples were studied by a JEOL-2010 high-resolution electron microscope. The FT-IR spectra were measured by a Magra-IR 750 Fourier transform infrared spectrometer after dispersing the samples in KBr pellet. The excitation spectra in UV and VUV range were measured at Beijing synchrotron radiation facility (BSRF). Ar^+ laser with wavelength at 514.5 nm and a fourth-order harmonic of YAG:Nd laser at 266 nm were used as a light source for emission spectra and decay curve measurement. The photoluminescence was analyzed by a Jobin–Yvon HRD-1 monochromator and detected by an R456 photomultiplier. All the spectra were measured at room temperature.

3. Result and discussion

3.1. Structure analysis

Fig. 1 shows the X-ray diffraction pattern of CS-made Lu_2O_3:Eu powders. Although there is an obvious broadening of the diffraction peaks as the G/N decreases, especially in sample D, all samples are of the same structure with the JCPDS card No. 43-1021 (also shown in Fig. 1 as a reference), from which we know that the samples crystallize in the cubic structure. From this pattern we can analysis the grain size D by Scherrer's formula:

$$D = \frac{0.89\,\lambda}{B\cos\,\theta}, \quad (2)$$

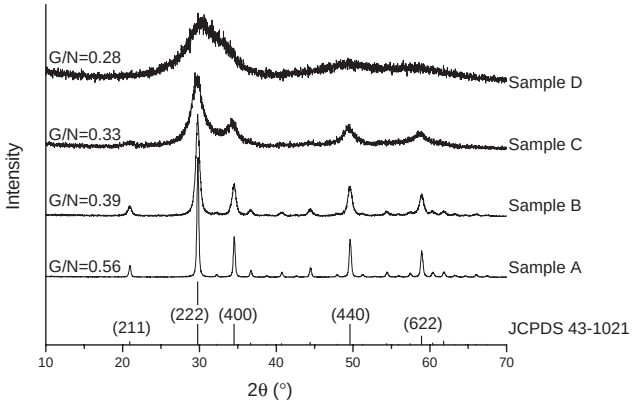

Fig. 1. XRD of CS-made nanocrystalline Lu_2O_3:Eu with different G/N.

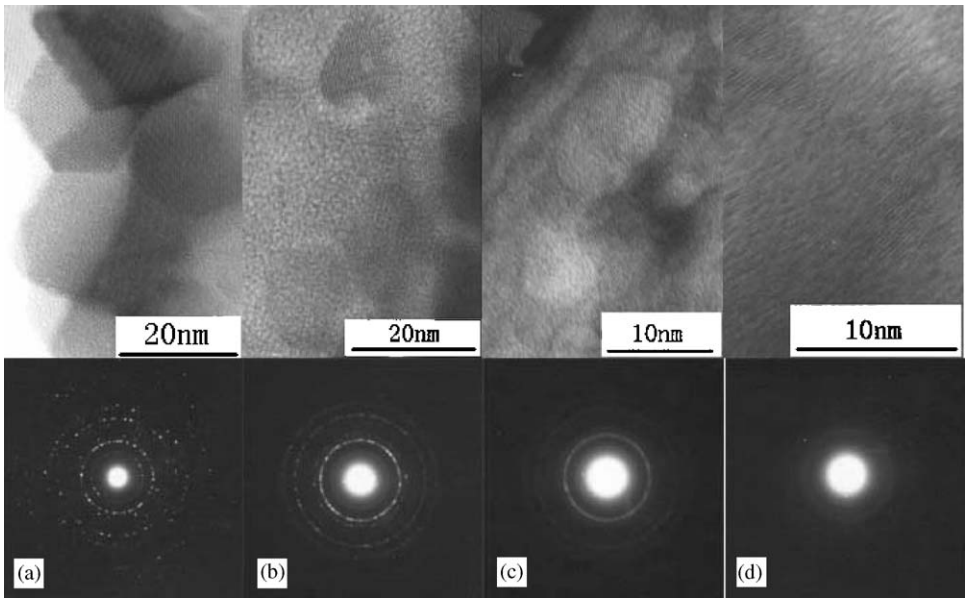

Fig. 2. HREM photographs of CS-made nanocrystalline Lu_2O_3:Eu: (a) sample A, 40 nm, (b) sample B, 15 nm, (c) sample C, 5 nm, (d) sample D, <5 nm.

where λ is the wavelength of Cu $K\alpha$ radiation, B is the corrected FWHM (radian) of diffraction peak, and θ is the diffraction angle. The calculated particle size of samples A, B, C is about 40, 15 and 5 nm, respectively. Because of the great broadening of the diffraction peaks in sample D, it is difficult to estimate its grain size merely by Scherrer's formula.

Fig. 2 presents HREM and electron diffraction (ED) images of samples A, B, C and D. The crystalline grains are spherical-like and the average size is almost the same as the one calculated by Scherrer's formula from XRD pattern. Moreover, from the HREM photo of sample D, one can learn that the particle size of the sample is less than 5 nm. These images show that our Lu_2O_3:Eu nanopowder consists of two structural components: one is well crystallized 'core' with long-range order, another is the amorphous grain boundary, especially in small size samples C and D. In general, as the particle size decreases the relative amount of amorphous phase increases. More surface defects can be seen in the images of samples C and D compared with that of samples A and B. As we will see later, this amorphous phase influences the luminescent properties greatly. The ED patterns give the same result: with the decrease of the particle size, the ED patterns vary from unorderly spots to polycrystalline diffraction circles.

The FT-IR spectra of samples A and D are shown in Fig. 3. The absorption peaks at 391, 494 and 578 cm^{-1} are due to Lu–O bond vibration in Lu_2O_3. The band around 1640 and 3420 cm^{-1} is ascribed to the vibration of O–H in H_2O, which is adsorbed by the sample itself and the dispersant KBr in the pellet during the process of measurement. The narrow peak at 1384 cm^{-1} is due to the residue NO_3^- in the sample, which can be easily

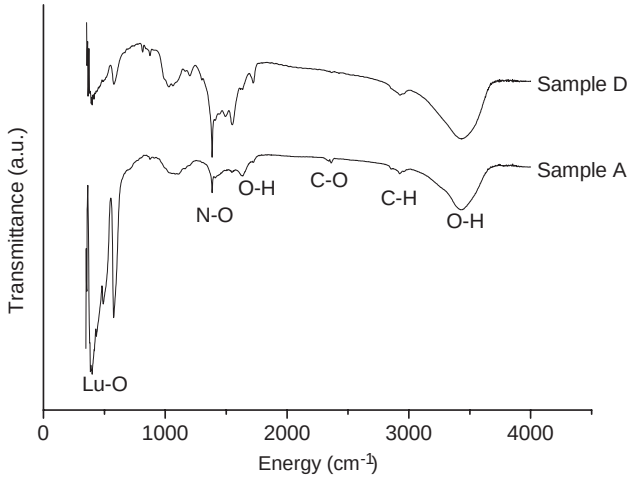

Fig. 3. FT-IR spectra of CS-made nanocrystalline Lu_2O_3:Eu: (a) sample A, G/N = 0.56, (b) sample D, G/N = 0.28.

removed after sintering at 500 °C for 1 h. Absorption band from 950 to 1200 cm^{-1} is supposed to be related with two-phonon processes, which should be confirmed by further experiments. By comparing these two curves, it is easy to notice that sample D, which is the oxidant-rich system, has more residue NO_3^-, while the vibration of Lu–O bond is not as intense as that in sample A. This result confirms the analysis from XRD patterns and HREM photographs.

3.2. Photoluminescence

The emission spectra under 514.5 nm excitation of CS-made Lu_2O_3:Eu are shown in Fig. 4a. All the spectra feature the typical emission of Eu^{3+} ion in cubic

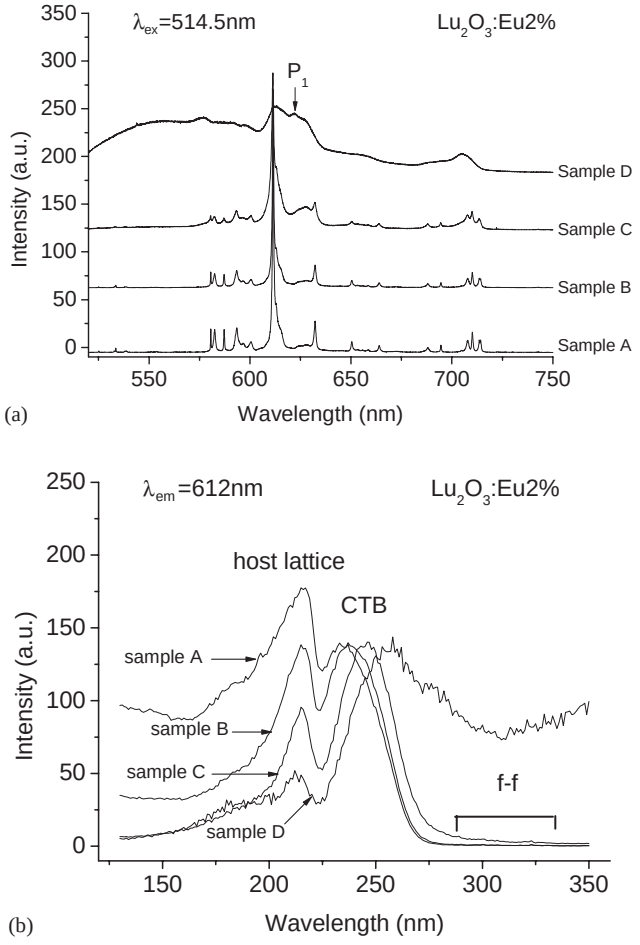

Fig. 4. Emission (a) and excitation (b) spectra of CS-made nanocrystalline Lu_2O_3:Eu 2% with different size.

structure [12]. The emission peaks of the samples with smaller particle size broaden greatly compared with bigger ones. Moreover, besides the normal emission from Eu^{3+} at C_2 and S_6 sites typically in Lu_2O_3 [13], there is a novel emission band around 622 nm (band P_1 in Fig. 4a), which might come from additional phase or site in nanoscale Lu_2O_3:Eu. It has been mentioned that samples obtained from combustion synthesis are very porous with particularly large surface area. This leads to the formation of a "fuzzy" interface of the nanoparticles, especially for sample D. Therefore, it seems to us that the extra band of sample D are resulted from Eu^{3+} ions located in the amorphous interface [14]. This supposition is supported by the fact that the relative intensities of these wide bands increase as the particle size decreases.

Fig. 4b is the excitation spectrum of the same samples in UV and VUV range, monitored at 612 nm line from the $^5D_0 \rightarrow {}^7F_2$ transition of Eu^{3+}. The relatively weak peaks above 280 nm originate in the *f–f* transition of Eu^{3+}. Similar to the result of Eu^{3+} ions in Y_2O_3 and Gd_2O_3, the band centered around 240–260 nm is assigned to the O^{2-}–Eu^{3+} charge transfer band (CTB). We have also measured the excitation spectra of Lu_2O_3 doped with other RE ions (Tb^{3+}, Er^{3+}, Dy^{3+}) (the spectra are not given here), and found that the band around 210 nm can be observed in all of the samples, suggesting that the band is due to the host absorption of Lu_2O_3 host lattice.

In order to investigate the excitation mechanism of nanocrystalline samples with different grain sizes, the excitation spectra were normalized by the intensity of CTB in this figure. It is worth to notice that the intensity of excitation peak of host lattice decreases greatly when the particle size decreases. To understand the result well, it's necessary to take a look at the feature of combustion synthesis. In the combustion process to produce small particles, such as for samples C and D, the flame temperature is much lower than that of bigger ones. The host lattice is far from 'perfect' and there are lots of defects both inside the particle and on the grain boundaries. As what we have seen in the HREM photographs, the small size samples are more "amorphous" compared to bigger ones. The foamy and porous products may adsorb some small molecules such as CO_2 and H_2O from the air. All these defects and impurities act as quenching center in the luminescence process. As a result, the excitation energy absorbed by the host may be transferred easily not to the activator ions but to the defects in small size samples.

Another thing should be noted is that the CTBs have an obvious red-shift in small particle samples compared with bigger ones. It is the energy of Eu–O bond that influences the charge transfer process. In nanoscale samples, especially very tiny ones, the host lattice is imperfect and incompact. Thus, the energy of Eu–O bond decreases and the binding energy of O^{2-} to the charge weakens. So it becomes easier for O^{2-} ions to transfer one charge to Eu^{3+}, resulting in the CTB shift to the lower energy side in smaller size samples. We have observed the same phenomenon in nanoscale Y_2O_3:Eu and Gd_2O_3:Eu powders[10,11].

3.3. Lifetime

To analyze the non-radiative relaxation among $^5D_J (J = 3, 2, 1, 0)$ of Eu^{3+}, decay curves of samples A, B, C and D were measured (Fig. 5). The lifetime of ^5D_J is obtained by fitting the curves and listed in Table 1 (the rise-processes in the decay curves and the slow component of about 4 ms of S_6 symmetric site [15] are not under consideration here). It is clear that for every energy level, the lifetime of small size sample is much shorter than that of bigger one. Some of them are even too fast to be measured due to the limitation of our equipment.

Generally, there are two paths for the excited ions relax to the lower or ground state: radiative process and

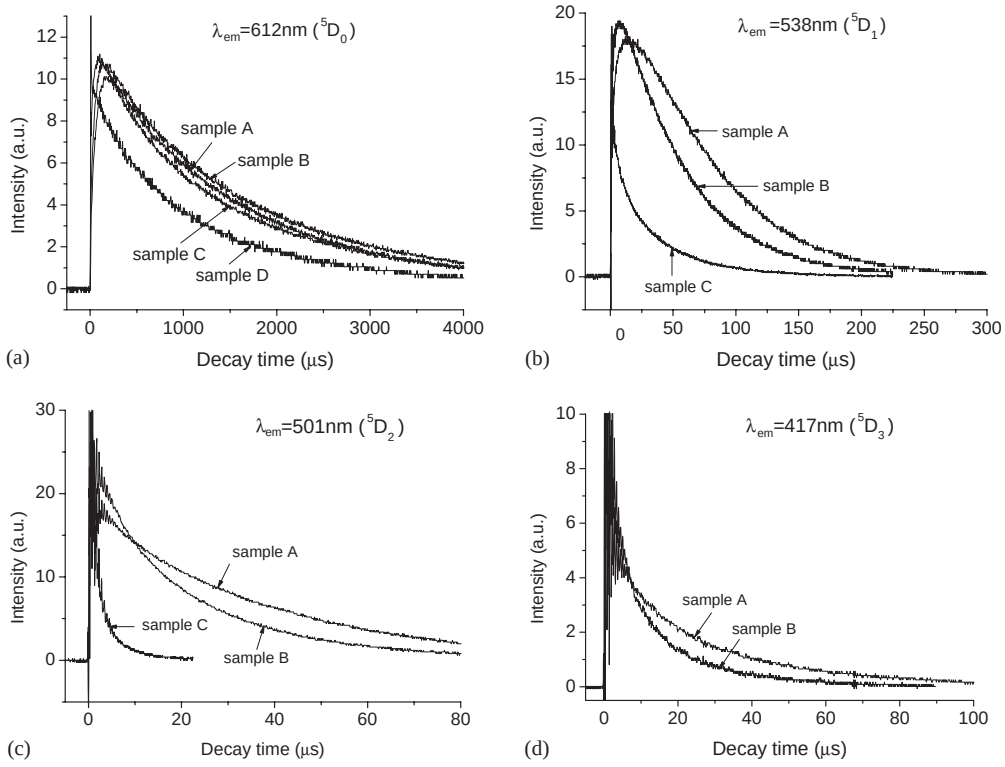

Fig. 5. Fluorescence decay curves of $^5D_{3,2,1,0}$ levels in Eu^{3+} ions for different samples, $\lambda_{ex} = 266$ nm.

Table 1
Lifetime of $^5D_0$, $^5D_1$, $^5D_2$ and $^5D_3$ levels in Eu^{3+} ions for different samples

	Energy level	$^5D_0$	$^5D_1$	$^5D_2$	$^5D_3$
Lifetime (μs)	Sample A (40 nm)	2000	59	36	32
	Sample B (15 nm)	2000	52	25	19
	Sample C (5 nm)	1900	44	5	—
			24	2	
	Sample D (<5 nm)	1500	—	—	—

non-radiative process. The lifetime τ is related to the decay rate of these two processes as follows:

$$\tau = (\gamma_r + \gamma_{nr})^{-1}. \quad (3)$$

When the particle size decreases, there are more and more defects and/or impurities acting as the quenching center in the samples. The excitation energy of RE ion may be transferred to these quenching centers very quickly. As a result, the decay rate of non-radiative process γ_{nr} increases and thus the lifetime τ decreases.

Another noteworthy result is that the decay curves of $^5D_{1,2}$ of sample C (5 nm) can no longer be fitted by single exponent. An additional component with a shorter lifetime of about 24 μs for $^5D_1$ and 2 μs for $^5D_2$ is present. From the analysis above, one can suppose that the short lifetime component is related to the amorphous phase and surface phase of the sample. Similar phenomena were also observed in some other nanoscale materials [14,16].

At the same time, we found that calcination process can lengthen the lifetime of the energy levels. This is obviously because that after calcination the powder becomes more compact and the surface state is improved by getting rid of adsorbed CO_2 and H_2O. As a result, the non-radiation caused by quenching centers decreases and the lifetime becomes longer.

4. Conclusion

Nanocrystalline Lu_2O_3:Eu were prepared by glycine-nitrate solution combustion synthesis. The excitation peaks show broadening and red-shift with the decreasing of particle size from 40 nm to less than 5 nm. The relative intensity of the excitation peaks of host lattice and CTB also changes with the particle size. In emission spectra, sample with small size shows great difference from bigger ones. The lifetime of ^5D_J decreases with the particle size. A new luminescent component due to Eu^{3+} ion locates at the amorphous phase is observed and analyzed.

Acknowledgments

This project is supported by The National High Technology Research and Development Program of China (863 Program) (No. 2002 AA 324070) and the

National Nature Science Foundation of China (No. 50332050).

References

[1] M.J. Weber, J. Lumin. 100 (2002) 35–45.
[2] D.W. Cooke, B.L. Bennett, R.E. Muenchausen, J.-K. Lee, M.A. Nastasi, J. Lumin. 106 (2004) 125–132.
[3] E. Zych, C. Brecher, A. Lempicki, Spectrochim. Acta, Part A: Mol. Bilmol. Spectrosc. 54 (1998) 1763–1769.
[4] C. Brechera, R.H. Bartramb, A. Lempickia, J. Lumin. 106 (2004) 159–168.
[5] R.H. Bartrama, A. Lempicki, L.A. Kappers, D.S. Hamilton, J. Lumin. 106 (2004) 169–176.
[6] E. Zych, P.J. Deren, W. Strek, A. Meijerink, W. Mielcarek, K. Domagala, J. Alloys Compd. 323–324 (2001) 8–12.
[7] E. Zych, D. Hreniak, W. Strek, L. Kepinski, K. Domagala, J. Alloys Compd. 341 (2002) 391–394.
[8] A. Lempicki, C. Brecher, P. Szupryczynski, H. Lingertat, V.V. Nagarkar, S.V. Tipnis, S.R. Miller, Nucl. Instrum. Methods Phys. Res. Sect. A 488 (2002) 579–590.
[9] W.P. Zhang, P.B. Xie, C.K. Duan, K. Yan, M. Yin, L.R. Lou, S.D. Xia, J.C. Krupa, Chem. Phys. Lett. 292 (1998) 133–136.
[10] Y. Tao, G.W. Zhao, W.P. Zhang, S.D. Xia, Mater. Res. Bull. 32 (1997) 501–506.
[11] P.B. Xie, W.P. Zhang, M. Yin, Y. Tao, S.D. Xia, Chin. J. Inorg. Mater. 13 (1998) 53–58.
[12] N.C. Chang, J.B. Gruber, J. Chem. Phys. 41 (1964) 3227–3234.
[13] E. Zych, M. Karbowiak, K. Domagala, S. Hubert, J. Alloys Compd. 341 (2002) 381–384.
[14] W.W. Zhang, M. Xu, W.P. Zhang, M. Yin, Z.M. Qi, S.D. Xia, C. Garapon, Chem. Phys. Lett. 376 (2003) 318–323.
[15] L. Ozawa, H. Forest, P.M. Jaffe, G. Ban, J. Electrochem. Soc. 118 (1971) 482–486.
[16] A.A. Bol, A. Meijerink, Phys. Rev. B: Condens. Matter 58 (1998) 15997–16000.